Condensate fraction of asymmetric three-component Fermi gas*

Du Jia-Jia(杜佳佳)[a], Liang Jun-Jun(梁军军)[b], and Liang Jiu-Qing(梁九卿)[a]†

[a] *Institute of Theoretical Physics, Shanxi University, Taiyuan* 030006, *China*
[b] *Department of Physics, Shanxi University, Taiyuan* 030006, *China*

(Received 6 March 2013; revised manuscript received 16 July 2013; published online 10 December 2013)

In this paper, we investigate the condensate fraction (CF) of fermionic pairs in the BCS–BEC crossover for three-component Fermi gas with both asymmetric interactions and unequal chemical potentials in two-dimensional free space. By using the functional-path-integral method, we have analytically derived the number densities and bound-state energy, from which the off-diagonal long-range order is analyzed in terms of the asymptotic behavior of the two-body density matrix. The explicit formula of CF is obtained as a function of the bound-state energy and population imbalance. It is demonstrated that the CF spectrum with respect to the bound-state energy can be used to characterize the quantum phase transition between the two kinds of Sarma phases as well as the transition from three-component to two-component superfluid. Moreover we obtain the same analytic formula of CF in the BCS superfluid phase as that of homogeneous Fermi gas with equal chemical potentials.

Keywords: condensate fraction, BCS–BEC crossover, Sarma phases

PACS: 03.75.Hh, 03.75.Ss, 05.30.Fk, 74.20.Fg **DOI:** 10.1088/1674-1056/23/2/020308

1. Introduction

In recent years, the crossover from Bardeen–Cooper–Schrieffer (BCS) superfluid of Fermi-pairs to the Bose–Einstein condensate (BEC) of molecular dimmers in ultracold Fermi gas (FG) has attracted considerable attention both experimentally[1–6] and theoretically.[7–18] The development of Feshbach-resonance technique allows the manipulation of two-particle interaction in a wide range, which is crucial in practical experiments to generate the Fermi-pairs and the crossover. It has been demonstrated that the population balance and imbalance in the crossover for two-component FG in two-dimensional (2D)[19–24] and three-dimensional (3D) free-spaces[25–30] resulted from the unequal particle-numbers in different components, which may lead to the mismatch of Fermi surfaces.

The spontaneous population imbalance in the crossover, first noted in Ref. [31], is an important feature of the three-component FG, in which it was also shown recently that the paring asymmetry can be generated in a uniform three-component FG with $U(3)$ interaction-symmetry.[32] It is demonstrated in Refs. [32] and [33] that the BCS superfluidity and population imbalance can coexist in the weak-coupling region, where the three-component superfluidity has been realized already with the lowest three hyperfine spin-states in the mixture of ^{6}Li atoms. The phase diagrams of three-component FG have been also investigated in 2D[34–36] and 3D[37] free-spaces.

The condensate fraction (CF) plays an important role in identification of the phase-diagram asymmetry. Moreover, the experimental results of the CF in the BCS–BEC crossover for ultracold two-component FG is shown to be in good agreement with the mean-field theoretical predictions[37,38] and Monte Carlo simulations.[39]

Ultracold quantum FG with tunable interactions provides a playground to generate the BCS–BEC crossover[40] experimentally, in which both fermionic and bosonic superfluidities can be studied in a unified manner. For imbalance FG, some exotic features appear, such as breached pairing-state (or Sarma superfluidity)[41] and the LOFF phase[42,43] (suggested by Larkin, Ovchinnikov, Fulde, and Ferrell). The Sarma phase is a spatially uniform state characterized by the coexistence of both superfluid and normal FGs, which, as a matter of fact, is accumulated in different regions of the momentum space forming a phase separation of shell structure with a superfluid core-region surrounded by a normal phase. Two kinds of breached pairing states are considered in this paper: P1 phase (in which the normal-phase region is bounded by a Fermi-surface) and P2 phase (in which the normal-phase region is located between two Fermi-surfaces). The two Sarma-phases have been predicted theoretically but have not yet been detected experimentally.

The quantum phase transition (QPT) usually refers to the structure change of ground state (at zero temperature) in many-body systems induced by the variation of interaction parame-

*Project supported by the Graduate Outstanding Innovation Item of Shanxi Province, China (Grant No. 20123005) and the National Natural Science Foundation of China (Grant Nos. 11075099 and 11275118).

†Corresponding author. E-mail: jqliang@sxu.edu.cn

© 2014 Chinese Physical Society and IOP Publishing Ltd

ters. The QPTs between two Sarma phases and between two types of superfluids have not resulted from symmetry breaking but have resulted from the Fermi-surface changes. It is remarkable to notice that, for the asymmetric three-component FG with the unequal chemical potentials, which are crucial to generate the Sarma superfluidity, the CF of BCS superfluid phase obtained in this paper has exactly the same formula as that in Ref. [34], where the chemical potentials of the three-components are equal.

It is believed that the CF of fermionic pairs is a signature of the superfluid phase in the BCS–BEC crossover.[44,45] Hence, measuring of CF experimentally makes it possible to search for clear evidence of the breached paring phases, namely the Sarma-phases. In this paper, we investigate the CF in the BCS–BEC crossover for the three-component FGs with both the asymmetric interactions and unequal chemical potentials in 2D free-space. Analytic results of the bound-state energy are obtained with the functional path-integral method and the CF of fermionic pairs is found in terms of the off-diagonal long-range order. We pay particular attention to the characteristic behaviors of CF in the two kinds of breached pairing-states in order to realize the asymmetric-interaction-induced Sarma superfluidity and related QPTs.

2. Model and formalism

The three-component FG can be described with the Hamiltonian

$$H=\sum_{\boldsymbol{k},i=R,G,B}\xi_{\boldsymbol{k},i}\psi^{\dagger}_{\boldsymbol{k},i}\psi_{\boldsymbol{k},i}+\sum_{\boldsymbol{k},\boldsymbol{k}',\boldsymbol{q},i,j}g_{i,j}b^{\dagger}_{\boldsymbol{k},\boldsymbol{q}}b_{\boldsymbol{k},\boldsymbol{q}'}, \tag{1}$$

where $\psi^{\dagger}_{\boldsymbol{k},i}$ is the creation field operator of color-index $i=R,G,B$ and momentum $\boldsymbol{k}$ in the convention that $\hbar=1$ throughout. $\xi_{\boldsymbol{k},i}=\varepsilon_{\boldsymbol{k},i}-\mu_{\boldsymbol{k},i}$ with $\varepsilon_{\boldsymbol{k}}=k^2/(2m)$ being the kinetic energy and $\mu_{\boldsymbol{k},i}$ the chemical potential of the fermionic component i. The interaction operator is defined by $b^{\dagger}_{\boldsymbol{k},q}=\psi^{\dagger}_{\boldsymbol{k}+\boldsymbol{q}/2,i}\psi^{\dagger}_{-\boldsymbol{k}+\boldsymbol{q}/2,j}$ $(i\neq j)$, where the parameter g is a negative value denoting the attractive interatomic interaction. We assume that the pairing only takes place between two components, say, the red and green particles, while the blue particles are not paired. Then, the Hamiltonian can be rewritten as

$$\begin{aligned}H=&\sum_{\boldsymbol{k},i=R,G,B}\xi_{\boldsymbol{k},i}\psi^{\dagger}_{\boldsymbol{k},i}\psi_{\boldsymbol{k},i}\\&+\sum_{\boldsymbol{k},\boldsymbol{k}',\boldsymbol{q}}g_{R,G}\psi^{\dagger}_{\boldsymbol{k}+\boldsymbol{q}/2,R}\\&\times\psi^{\dagger}_{-\boldsymbol{k}+\boldsymbol{q}/2,G}\psi_{-\boldsymbol{k}'+\boldsymbol{q}/2,G}\psi_{\boldsymbol{k}'+\boldsymbol{q}/2,R}.\end{aligned} \tag{2}$$

We begin with the partition function

$$Z=\int D\phi D\phi^{*}\exp(-S[\phi,\phi^{*}]) \tag{3}$$

with the action defined by

$$S[\phi,\phi^{*}]=\int_0^{\beta}\mathrm{d}\tau\left[\sum_{\boldsymbol{k},i}\psi^{\dagger}_{\boldsymbol{k},i}(\tau)(\partial_{\tau}-\mu)\psi_{\boldsymbol{k},i}(\tau)+H\right]. \tag{4}$$

Using the Hubbard–Stratonovitch transformation with auxiliary field $\phi_{\boldsymbol{k}}(\tau)=\Delta\delta_{\boldsymbol{k},0}+\eta_{\boldsymbol{k}}(\tau)$, the Fermi field can be integrated out under Gauss approximation, and the partition function becomes $Z=\int D\Delta D\Delta^{*}\exp(S_{\mathrm{eff}})$. The effective action can be approximated as

$$S_{\mathrm{eff}}=S_0[\Delta]+\frac{1}{2}\sum_{q}\bar{\eta}^{\dagger}(q)M(q)\bar{\eta}(q), \tag{5}$$

where

$$S_0=\beta\frac{\Delta^2}{g}-\sum_{k}\mathrm{Tr}\ln\left[\boldsymbol{G}_0(k)/\beta\right]^{-1}, \tag{6}$$

is the saddle-point action and Δ denotes the energy-gap, which is regarded as an order-parameter of the FG. $G_0^{-1}(k)$ is the inverse fermion propagator with $\beta=1/k_{\mathrm{B}}T$ as usual, $k=(k,\omega_n)$, and $\omega_n=(2n+1)\pi/\beta$ is the fermionic Matsubara frequency. The second term in the effective action S_{eff} stands for the Gaussian correction, where $\eta(q)$ in the vector $\bar{\eta}^{\dagger}=[\eta^{*}(q),\eta(-q)]$ denotes the small deviation from the saddle point solution with $q\equiv(q,\mathrm{i}w_m)$ and $w_m=2m\pi/\beta$ is the Bosonic Matsubara frequency. In this paper, we do not consider the sound velocity, so the elements of fluctuation matrix $M(q)$ are not given. The saddle-point thermodynamical potential is $\Omega_0=S_0\left[\Delta_0\right]/\beta$, which can be written explicitly as[46]

$$\begin{aligned}&\Omega_0\left(\Delta,\mu_R,\mu_G,\mu_{\mathrm{B}}\right)\\&=\sum_{\boldsymbol{k}}\Big[f(E_{\boldsymbol{k},+})E_{\boldsymbol{k},+}+f(E_{\boldsymbol{k},-})E_{\boldsymbol{k},-}\\&\quad+\xi_{\boldsymbol{k},G}-E_{\boldsymbol{k},-}+f_{\mathrm{F}}\left(\mu_{\mathrm{B}}\right)\xi_{\boldsymbol{k},B}-\frac{\Delta^2}{g}\Big],\end{aligned} \tag{7}$$

where $f_{\mathrm{F}}(x)=[\exp(\beta x)+1]^{-1}$ is the Fermi distribution function. $E_{\boldsymbol{k},\pm}=(\xi^2_{\boldsymbol{k},+}+\Delta^2)^{1/2}\pm\xi_{\boldsymbol{k},-}$ denote the quasiparticle and the quasihole energies, where $\xi_{\boldsymbol{k},\pm}=(\xi_{\boldsymbol{k},R}\pm\xi_{\boldsymbol{k},G})/2=k^2/(2m)-\mu_{\pm}$. The effective chemical potentials $\mu_{\pm}=(\mu_R\pm\mu_G)/2$ indicate the chemical potential imbalance between red and green particles. The particle number of color-index i is given by $N_i=-\partial\Omega/\partial\mu_i$, where $\Omega=\Omega_0+\Omega_{\mathrm{fluc}}$ is the thermodynamical potential including the fluctuation part. The particle number contributed from the Gaussian fluctuation

$$N_{\mathrm{fluct},i}=-(1/\beta)\sum_{q}\{\partial[\det\boldsymbol{M}(q)]/\partial\mu_i\}/\det\boldsymbol{M}(q) \tag{8}$$

vanishes in the zero-temperature limit, $T\to 0$. The saddle-point approximation of particle number is then obtained from

the variation $N_{0,i} = -\partial\Omega_0(\Delta,\mu_R,\mu_G,\mu_B)/\partial\mu_i$, and the explicit formulas of the three-color particle-number densities $n_i = N_{0,i}/V$ are given, respectively, by

$$n_R = \int \frac{\mathrm{d}^2\boldsymbol{k}}{(2\pi)^2}\left[(1-f(E_{\boldsymbol{k},-}))v_{\boldsymbol{k}}^2 + f(E_{\boldsymbol{k},+})u_{\boldsymbol{k}}^2\right], \quad (9)$$

$$n_G = \int \frac{\mathrm{d}^2\boldsymbol{k}}{(2\pi)^2}\left[(1-f(E_{\boldsymbol{k},+}))v_{\boldsymbol{k}}^2 + f(E_{\boldsymbol{k},-})u_{\boldsymbol{k}}^2\right], \quad (10)$$

$$n_B = \int \frac{\mathrm{d}^2\boldsymbol{k}}{(2\pi)^2}\left[f_F(\mu_B)\right], \quad (11)$$

where $u_{\boldsymbol{k}}^2 = (1+\xi_{\boldsymbol{k},+}/E_{\boldsymbol{k}})/2$, $v_{\boldsymbol{k}}^2 = (1-\xi_{\boldsymbol{k},+}/E_{\boldsymbol{k}})/2$, and $E_{\boldsymbol{k}} = (E_{\boldsymbol{k},+}+E_{\boldsymbol{k},-})/2$. The number equations (9) and (10) of paired components are coupled with the gap equation

$$-\frac{1}{g} = \frac{1}{V}\sum_{\boldsymbol{k}}\frac{1-f(E_{\boldsymbol{k},+})-f(E_{\boldsymbol{k},-})}{2\sqrt{\xi_{\boldsymbol{k},+}^2+\Delta^2}}, \quad (12)$$

which is obtained from the minimum variation-principle of the thermodynamic potential with respect to the energy-gap Δ such that $\delta S_0/\delta\Delta = 0$, ($S_0 = \beta\Omega_0$). In this paper, the bound-state energy ϵ_B, rather than interaction strength g is used to describe the BCS–BEC crossover. By combining the contact potential equation

$$-\frac{1}{g} = \frac{1}{V}\sum_{\boldsymbol{k}}\frac{1}{k^2/m+\epsilon_B}, \quad (13)$$

in which the bound-state energy ϵ_B is introduced, and the gap equation (12), the interaction strength g can be eliminated and we have

$$\sum_{\boldsymbol{k}}\left(\frac{1-f(E_{\boldsymbol{k},+})-f(E_{\boldsymbol{k},-})}{2\sqrt{\xi_{\boldsymbol{k},+}^2+\Delta^2}}\right) = \sum_{\boldsymbol{k}}\left(\frac{1}{k^2/m+\epsilon_B}\right). \quad (14)$$

In the following, we shall consider only the zero-temperature limit $T\to 0$ and, thus, the Fermi distribution function $f(E_{\boldsymbol{k},\pm})$ in the above equations can be substituted by $\theta(-E_{\boldsymbol{k},\pm})$, where $\theta(x)$ is the Heaviside step function with $f(x) = 0$ for $x < 0$ and $f(x) = 1$ for $x \geq 0$. The explicit formulas of gap parameter and chemical potentials are derived from the coupled equations (9), (10), and (14) for asymmetric three-component FG in order to describe the BCS–BEC crossover.

For the sake of convenience, we choose the single-particle kinetic energy $\varepsilon_{\boldsymbol{k}} = k^2/(2m)$ as the integral variable. The quasiparticle energy zeros ε_r with $r = 1,2$ are easily obtained as

$$\varepsilon_r = \mu_+ + (-1)^r\sqrt{\mu_-^2-\Delta^2} \quad (15)$$

with two momenta defined by $k_r = \sqrt{2m\varepsilon_r}$. In the chemical potential range $|\mu_-| > \Delta$, $\varepsilon_1 < 0$, and $\varepsilon_2 > 0$, there is only one energy zero-point. The normal state of red component is in the central part of momentum space and superfluid phase is on the borders of k_2. While there are two zero-points in the chemical potential range $|\mu_-| > \Delta$, $\varepsilon_1 > 0$, and $\varepsilon_2 > 0$, where the pairing occurs around the lower and higher Fermi surfaces for k_1 and k_2, respectively. The two regions are separated by the gapless excitation. In the chemical potential range $-\Delta < \mu_- < \Delta$, we have the BCS superfluid state since the zero-point energy ε_r becomes complex and, thus, the quasiparticle energies $E_{\boldsymbol{k},+}$ and $E_{\boldsymbol{k},-}$ are positive.

The condensed particle-number in interacting many-body systems is strictly related to the off-diagonal long-range order (ODLRO), which was proposed in terms of the two-body density matrix[47] defined as $\rho(r_R',r_G',r_R,r_G) \equiv \langle\psi_R^\dagger(\boldsymbol{r}_R')\psi_G^\dagger(\boldsymbol{r}_G')\psi_R(\boldsymbol{r}_R)\psi_G(\boldsymbol{r}_G)\rangle$, where $\psi_i(r)$, $\psi_i^\dagger(r)$ are, respectively, the fermionic creation, annihilation operators of the i-th species in the position r and the notation $\langle\cdots\rangle$ stands for quantum mechanical expectation-value. For a homogeneous FG, the ODLRO of Fermi superfluid is characterized by the asymptotic behavior of density matrix $\rho(r_R',r_G',r_R,r_G)$ in the limit $|\boldsymbol{r}_R-\boldsymbol{r}_R'|, |\boldsymbol{r}_G-\boldsymbol{r}_G'| \to \infty$. While the largest eigenvalue of the density matrix gives rise to the number of Fermi pairs in the BEC phase denoted by

$$N_c = \int \mathrm{d}^2\boldsymbol{r}_R\mathrm{d}^2\boldsymbol{r}_G\left|\langle\psi_R(\boldsymbol{r}_R)\psi_G(\boldsymbol{r}_G)\rangle\right|^2, \quad (16)$$

which can be transformed as[48]

$$N_c = \int \frac{\mathrm{d}^2\boldsymbol{k}}{(2\pi)^2}u_k^2v_k^2. \quad (17)$$

In this paper, we define a physical quantity called population imbalance that[36]

$$P = \frac{n_R-n_G+n_B}{n} \quad (18)$$

with the particle-number equation defined by

$$n = n_R+n_G+n_B = m\epsilon_F/\pi, \quad (19)$$

where ϵ_F is the Fermi energy. The population imbalance P with values in the range $[0,1]$ can be used to identify the phase transition, as seen in the following.

3. Sarma superfluid phases

The system is in Sarma phase when population imbalance does not vanish $P \neq 0$ and $E_{\boldsymbol{k},+} < 0$ in the region $[\varepsilon_1,\varepsilon_2]$, which can be divided to three cases: $0 < \varepsilon_1 < \varepsilon_2$, $\varepsilon_1 < 0 < \varepsilon_2$, and $\varepsilon_1 < \varepsilon_2 < 0$. The third case is known as the BCS superfluid phase from the above analysis and the other two are both the Sarma phases, which are denoted by P2 and P1, respectively. For the sake of simplicity, we let the chemical potential of the blue component be $\mu_B = \mu_+$ throughout the paper.

3.1. Sarma phase P2

The P2 phase at the BCS side of the crossover is localized in the pairing mode-region $k_1 < k < k_2$, where the quasiparticle energy is negative $E_{\boldsymbol{k},+} < 0$ and the quasihole energy is positive $E_{\boldsymbol{k},-} > 0$. The pairing occurs in the two regions around the lower (k_1) and higher (k_2) Fermi surfaces separated by the gapless excitation region. The bound-state energy is obtained as

$$\frac{\epsilon_{\rm B}}{\epsilon_{\rm F}} = \frac{3\left[\sqrt{x_0^2+1}-x_0\right]\left[\sqrt{y_0^2-1}+y_0\right]}{\left[x_0\theta(x_0)+x_0+\sqrt{x_0^2+1}\right]\left[y_0-\sqrt{y_0^2-1}\right]}, \quad (20)$$

where $\omega_r = \varepsilon_r/\Delta$, $x_0 = \mu_+/\Delta$, $\omega_r - x_0 = \pm\sqrt{y_0^2-1}$ with $y_0 = \mu_-/\Delta$. The population imbalance P is easily obtained from Eq. (18) as

$$P = \frac{x_0\theta(x_0)+2\sqrt{y_0^2-1}}{x_0\theta(x_0)+x_0+\sqrt{x_0^2+1}}. \quad (21)$$

Then, we can obtain the CF $n_{\rm c} = N_{\rm c}/V$ from Eq. (17) and the ratio with respect to the total particle-number density n is found as[36]

$$\frac{n_{\rm c}}{n} = \frac{1}{4}\frac{\left[\pi/2+\arctan(x_0)-2\arctan\left(\sqrt{(y_0)^2-1}\right)\right]}{x_0\theta(x_0)+x_0+\sqrt{x_0^2+1}}. \quad (22)$$

3.2. Sarma phase P1

The smallest thermodynamic potential is reached when the negative quasiparticle-energy modes are filled and the remaining modes are left empty. The P1 phase at the BEC side of the crossover is in the integral range $[0, \varepsilon_2]$ with the pairing modes $k > k_2$ and $E_{\boldsymbol{k},+} < 0$, $E_{\boldsymbol{k},-} > 0$. For the case $k_1 = 0$, the normal Fermi-state of redundant component is in the central part of momentum space of k_2 while the superfluid phase is on the borders. The bound-state energy is obtained as

$$\frac{\epsilon_{\rm B}}{\epsilon_{\rm F}} = \frac{3\left[\sqrt{y_0^2-1}+y_0\right]}{x_0\theta(x_0)+x_0+y_0}. \quad (23)$$

Similarly, we can find the population imbalance

$$P = \frac{x_0\theta(x_0)+x_0+\sqrt{y_0^2-1}}{x_0\theta(x_0)+x_0+y_0} \quad (24)$$

and the CF

$$\frac{n_{\rm c}}{n} = \frac{\left[\pi/2-\arctan\left(\sqrt{(y_0)^2-1}\right)\right]}{x_0\theta(x_0)+x_0+y_0}. \quad (25)$$

3.3. BCS superfluid phase

The system is in a BCS superfluid phase when both quansiparticle-energies are positive $E_{\boldsymbol{k},\pm} > 0$. In the chemical potential region $-\Delta < \mu_- < \Delta$, the particle number densities of the red and green components in this phase are equal, as seen from Eqs. (9) and (10). The bound-state energy is given by

$$\frac{\epsilon_{\rm B}}{\epsilon_{\rm F}} = \frac{3\left[\sqrt{x_0^2+1}-x_0\right]}{x_0\theta(x_0)+x_0+\sqrt{x_0^2+1}} \quad (26)$$

and the population imbalance P is

$$P = \frac{x_0\theta(x_0)}{x_0\theta(x_0)+x_0+\sqrt{x_0^2+1}}. \quad (27)$$

The superfluid phase considered in this paper is slightly different from the standard BCS state and describes a superposition of empty and occupied paired-states. Equation (17) gives rise to the CF expression[36]

$$\frac{n_{\rm c}}{n} = \frac{1}{4}\frac{[\pi/2+\arctan(x_0)]}{x_0\theta(x_0)+x_0+\sqrt{x_0^2+1}}, \quad (28)$$

which is exactly the same as that obtained in Ref. [34], where the chemical potentials of the three-component are equal.

4. CF and QPT

From the phase diagram given in Ref. [36] it is seen that the population imbalance reaches a value $P = 1/3$ in the BCS limit $(\epsilon_{\rm B}/\epsilon_{\rm F} = 0)$ for both the BCS superfluid and the Sarma phases. The critical point $x_0 = 0$, where $\epsilon_{\rm B}/\epsilon_{\rm F} = 3$ and $P = 0$, is a common point of the three phases. The Sarma phase P2 begins from $\epsilon_{\rm B}/\epsilon_{\rm F} = 0$ and extends to $\epsilon_{\rm B}/\epsilon_{\rm F} = 3$. With the increase of bound-state energy, the Sarma phases P2 and P1 appear in turn, which are separated by the critical line $P = 3 - \epsilon_{\rm B}/\epsilon_{\rm F}$. The unpaired blue-color component vanishes[34] at the critical point $\epsilon_{\rm B}/\epsilon_{\rm F} = 3$, where only two components (red and green) remain in the crossover. The main goal of this paper is to demonstrate that the QPT between P1 and P2 can be characterized by the CF $n_{\rm c}/n$ of Fermi pairs, which as a function of the scaled bound-state energy $\epsilon_{\rm B}/\epsilon_{\rm F}$ that is plotted in Fig. 1 for different values of the imbalance-ratio $P = 0.3, 0.5, 0.8$, respectively. It may be worthy to remark that there is no symmetry breaking for the transition between P1 and P2 but a change of fermionic excitation in the momentum space. The CF curves in the lower region of energy are referred to P2 and approach to the P1 phase with the increase of energy. $t_{0.3}$, $t_{0.5}$, and $t_{0.8}$ in Fig. 1 denote the critical points between the two types of Sarma phases P1 and P2. The CF in

the phase P2 decreases with the increase of the imbalance ratio P in agreement with the phase diagram,[36] where the bound-state energy ϵ_B/ϵ_F in phase P2 for $P = 0.8$ is smaller than that of $P = 0.3$. The CF vanishes in P2 at the bound-state energy value $\epsilon_B/\epsilon_F = 1$ for $P = 0.8$, which is consistent with the phase diagram, where the phase P2 appears only when $P = 0.8$ and $\epsilon_B/\epsilon_F = 1$. The CF in phase P1 grows very slowly with the energy unlike the BCS side, where it has a very fast growth and approaches asymptotically the imbalance-ratio-dependent values, where the unpaired number of Fermions becomes zero in the limit $\epsilon_B/\epsilon_F \to \infty$ or, in other words, all the minority Fermi-pairs are condensed in the BEC limit.

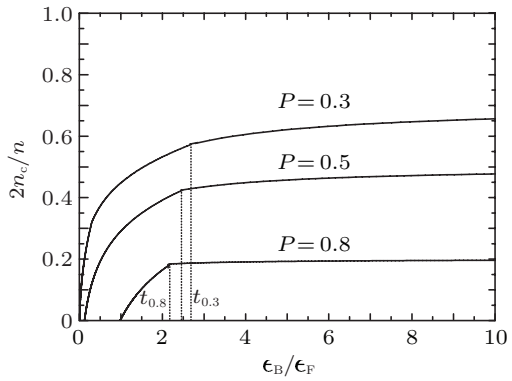


Fig. 1. CFs of Fermi pairs as a function of bound-state energy ϵ_B/ϵ_F for $P = 0.3$, $P = 0.5$, $P = 0.8$ with critical points of phase transition $t_{0.3}$, $t_{0.5}$, and $t_{0.8}$, respectively.

The CF in the BCS superfluid phase as a function of bound-state energy is plotted in Fig. 2, from which it is seen that the CF becomes zero when the bound-state energy ϵ_B/ϵ_F vanishes. A very small fraction of the fermions contribute to the Cooper-pair condensate in the BCS limit, since only the fermions near the Fermi surface form a Cooper-pair in the weak-coupling regime. At the critical point $\epsilon_B/\epsilon_F = 3$ the third component (blue) vanishes.[34] Below the critical point the superfluid contains three-component and becomes two-components above it. Thus, a sharp first-order QPT is recognized in terms of the CF spectrum, unlike the pure two-component case[36] where the transition from BCS to BEC limit is smooth. This QPT with the structure change of superfluids is obviously induced by the Fermi-surface variation. The Cooper-pair CF increases slowly with the bound-state energy above the critical point, where the fermion-pairs are bound to isolated molecules. In the energy limit $\epsilon_B/\epsilon_F \to \infty$, the CF approaches to a fixed value $n_c/n \to 1/2$, namely one half of the fermion-pair condensate.

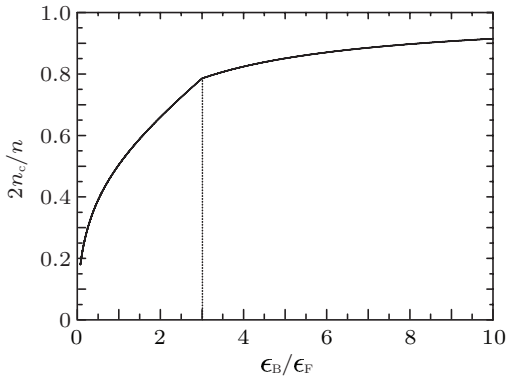


Fig. 2. CF as a function of bound-state energy in the superfluid phase, which contains three-components below the critical point $\epsilon_B/\epsilon_F = 3$ while two-components are above it.

5. Conclusions

The QPT in the BCS–BEC crossover has been investigated for the first time in terms of the CF for three-component Fermi gas with both the asymmetric interactions and unequal chemical potentials. The two kinds of Sarma phases and superfluids are well characterized by the CF spectrum with respect to the bound-state energy of Fermi-pairs. The Sarma phases resulted from the unequal chemical potentials while the two kinds of superfluids are due to the existence of the third component, which leads to an imbalance of the Fermi surfaces and, thus, affects the pairing. In the Sarma phase P2 (BCS side) CF grows fast with the increase of bound-state energy ϵ_B/ϵ_F, while in the P1 phase it approaches asymptotically a maximum value $(1-P)$ in the BEC limit. It is found that the CF behaviors are similar for the three-component (BCS side) and two-component superfluids. The QPTs for both Sarma phases and superfluids are seen to be the sharp first-order from the viewpoint of the CF spectrum.

References

[1] Jochim S, Bartenstein M, Altmeyer A, Hendl G, Riedl S, Chin C, Denschlag J H and Grimm R 2003 *Science* **302** 2101
[2] Greiner M, Regal C A and Jin D S 2003 *Nature* **426** 537
[3] Zwierlein M W, Abo-Shaeer J, Schirotzek A, Schunck C and Ketterle W 2004 *Nature* **435** 1047
[4] Zwierlein M W, Stan C A, Schunck C H, Raupach S M F, Gupta S, Hadzibabic Z and Ketterle W 2003 *Phys. Rev. Lett.* **91** 250401
[5] Zwierlein M W, Schirotzek A, Schunck C H and Ketterle W 2006 *Science* **311** 492
[6] Kinast J, Hemmer S L, Gehm M E, Turlapov A and Thomas J E 2004 *Phys. Rev. Lett.* **92** 150402
[7] Bloch I, Dalibard J and Zwerger W 2008 *Rev. Mod. Phys.* **80** 885
[8] Falco G M and Stoof H T C 2004 *Phys. Rev. Lett.* **92** 130401
[9] Hu H, Minguzzi A, Liu X J and Tosi M P 2004 *Phys. Rev. Lett.* **93** 190403
[10] Zhai H 2009 *Phys. Rev. A (Rapid Communication)* **80** 051605
[11] Cui X L and Zhai H 2010 *Phys. Rev. A (Rapid Communication)* **81** 041602
[12] Zhou Y, Ma X D and Huang G X 2006 *Chin. Phys. Lett.* **23** 2662
[13] Zhang W Y and Wang C T 2010 *Chin. Phys. Lett.* **27** 040304
[14] Huang B B and Wan S L 2009 *Chin. Phys. Lett.* **26** 070304
[15] Wang Y S, Yan P G, Li B and Liu X S 2012 *Chin. Phys. B* **21** 010309

[16] Ma Z Q and Yang C N 2009 *Chin. Phys. Lett.* **26** 120505
[17] Hao Y J 2011 *Chin. Phys. B* **20** 060307
[18] Chao G and Zhen H Y 2012 *Phys. Rev. A* **86** 043609
[19] He L Y and Zhuang P F 2008 *Phys. Rev. A* **78** 033613
[20] Conduit G J, Conlon P H and Simons B D 2008 *Phys. Rev. A* **77** 053617
[21] Marini M, Pistolesi F and Strinati G C 1998 *Eur. Phys. J. B* **1** 151
[22] Du J J, Chen C and Liang J J 2009 *Phys. Rev. A* **80** 023601
[23] Parish M M 2011 *Phys. Rev. A* **83** 051603
[24] Salasnich L 2007 *Phys. Rev. A* **76** 015601
[25] Iskin M and Sa de Melo C A R 2006 *Phys. Rev. Lett.* **97** 100404
[26] Iskin M and Sa de Melo C A R 2007 *Phys. Rev. A* **76** 013601
[27] Liu W V and Wilczek F 2003 *Phys. Rev. Lett.* **90** 047002
[28] Hu H and Liu X J 2006 *Phys. Rev. A* **73** 051603
[29] Pao C H, Wu S T and Yip S K 2006 *Phys. Rev. B* **73** 132506
[30] Su W C 2006 *Phys. Rev. A* **74** 063627
[31] He L Y, Jin M and Zhuang P F 2006 *Phys. Rev. A* **74** 033604
[32] Ozawa T and Baym G 2010 *Phys. Rev. A* **82** 063615
[33] Cherng R W, Refael G and Demler E 2007 *Phys. Rev. Lett.* **99** 130406
[34] Salasnich L 2011 *Phys. Rev. A* **83** 033630
[35] Salasnich L e-print arXiv: **1108** 0076
[36] Du J J, Liang J J and Liang J Q 2012 *Phys. Rev. A* **85** 033610
[37] Salasnich L, Manini N and Parola A 2005 *Phys. Rev. A* **72** 023621
[38] Ortiz G and Dukelsky J 2005 *Phys. Rev. A* **72** 043611
[39] Astrakharchik G E, Boronat J, Casulleras J and Giorgini S 2005 *Phys. Rev. Lett.* **95** 230405
[40] Regal C A, Greiner M and Jin D S 2004 *Phys. Rev. Lett.* **92** 040403
[41] Sarma G 1963 *J. Phys. Chem. Solids* **24** 1029
[42] Fulde P and Ferrell R A 1964 *Phys. Rev.* **135** A550
[43] Larkin A J and Ovchinnikov Y N 1964 *Zh. Eksp. Teor. Fiz.* **47** 1136 [1963 *Sov. Phys. JEPT* **20** 762]
[44] Zwierlein M W, Stan C A, Schunck C H, Raupach S M F, Kerman A J and Ketterle W 2004 *Phys. Rev. Lett.* **92** 120403
[45] Zwierlein M W, Schunck C H, Stan C A, Raupach S M F and Ketterle W 2005 *Phys. Rev. Lett.* **94** 180401
[46] Vivas H e-print arXiv: **0504** 600
[47] Yang C Y 1962 *Rev. Mod. Phys.* **34** 694
[48] Campbell C E, Clark J W and Panat P V 1997 *Condensed Matter Theories* (New York: Nova Science) Vol. **12**, p. 131